Ca^{2+}/calmodulin-dependent protein kinase kinase β phosphorylation of Sirtuin 1 in endothelium is atheroprotective

Liang Wen[a,b], Zhen Chen[b], Fan Zhang[c], Xiaopei Cui[b], Wei Sun[b], Greg G. Geary[d], Yinsheng Wang[c], David A. Johnson[b], Yi Zhu[a,1], Shu Chien[e,1], and John Y.-J. Shyy[b,f,1]

[a]Department of Physiology and Pathophysiology, Peking University Health Sciences Center, Beijing 100191, China; [b]Division of Biomedical Sciences and [c]Department of Chemistry, University of California, Riverside, CA 92521; [d]Department of Kinesiology and Health Sciences, California State University, San Bernardino, CA 92407; and Departments of [e]Bioengineering and [f]Medicine, University of California, San Diego, La Jolla, CA 92093

Contributed by Shu Chien, May 16, 2013 (sent for review March 3, 2013)

Atheroprotective flow exerts antioxidative and anti-inflammatory effects on vascular endothelial cells (ECs), in part through the induction of Sirtuin 1 (SIRT1), a class III histone deacetylase. The role of Ca^{2+}/calmodulin-dependent protein kinase kinase (CaMKK)β in flow induction of SIRT1 both in vitro and in vivo was investigated. Pulsatile shear stress mimicking atheroprotective flow increased the level of SIRT1 in cultured ECs by enhancing its stability, and this effect was abolished by inhibition or knockdown of CaMKKβ. Flow-enhanced SIRT1 stability was primarily mediated by CaMKKβ phosphorylation of SIRT1 at Ser-27 and Ser-47, as evidenced by in vitro kinase assay, mass spectrometry, and experiments using loss- or gain-of-function SIRT1 mutants. Flow-induced CaMKKβ phosphorylation of SIRT1 Ser-27 and Ser-47 increased antioxidative and anti-inflammatory capacities. Ablation of CaMKKβ or SIRT1 in mice with an apolipoprotein E-null background showed increased atherosclerosis both in athero-prone and in athero-protective areas. The results suggest that the CaMKKβ-SIRT1 axis in ECs is mechanosensitive, antioxidative, and anti-inflammatory.

Shear stress-imposed endothelial responses affect vascular physiology and pathophysiology. Ample evidence indicates that atheroprotective flow with pulsatile shear stress (PS) modulates endothelial homeostasis via antioxidative and anti-inflammatory effects on vascular endothelial cells (ECs). These beneficial effects are mediated in part by the induction of Sirtuin (SIRT)1 (1). Functioning as a class III histone deacetylase, SIRT1 modulates cellular functions through deacetylation of targets such as Forkhead box (Fox)O, peroxisome proliferator-activated receptor (PPAR)γ, PPARγ coactivator (PGC)1α, and nuclear factor kappa-light chain enhancer of activated B cells (NF-κB), which are involved in oxidative and inflammatory states of the cell (2). SIRT1 ablation in ECs blocks angiogenesis in vitro and in vivo (3), and transgenic mice with EC-specific SIRT1 overexpression show decreased atherosclerosis (4). Additionally, SIRT1 can deacetylate endothelial nitric oxide synthase (eNOS) to stimulate eNOS activity and increase NO production (5).

The expression of SIRT1 is controlled at multiple levels, including transcription, posttranscription, and posttranslation (6). Posttranslationally, the SIRT1 level and/or its activity can be modulated by sumoylation and phosphorylation (7, 8). Also, the mRNA stability of SIRT1 can be regulated by microRNAs (9, 10). More than 10 residues of SIRT1 are phosphorylated/dephosphorylated in multiple cell types under various conditions (7). Among these, Ser-27 and Ser-47 in human SIRT1 are the most studied. Several kinases, including c-Jun N-terminal kinase (JNK) 1, JNK2, mammalian target of rapamycin, and cyclin-dependent kinase 5 (CDK5), are implicated in the phosphorylation of Ser-27 and Ser-47 (11-14), but the functional consequence of their phosphorylation is unclear. None of the identified kinases involved in SIRT1 phosphorylation has been shown to respond to atheroprotective flow. Given the link between shear stress and SIRT1, there could be a flow-responsive cytoplasmic kinase that phosphorylates SIRT1 to enhance its activity.

Like SIRT1, AMP-activated protein kinase (AMPK) functions as a master regulator in stress response and energy homeostasis in eukaryotic cells. SIRT1 and AMPK are coregulated by caloric restriction, resveratrol, and exercise (15, 16), which coordinately deacetylate and phosphorylate a common set of molecular targets such as PGC1α (17). Because SIRT1 and AMPK are regulated in concert, a common upstream regulator is likely to exist. Considering that elevated AMPK activity requires the phosphorylation of Thr-172 in its α subunit by AMPK kinases (AMPKKs), an AMPKK might also phosphorylate SIRT1 to regulate its activity or expression. The probable kinases involved in such regulation are Ca^{2+}/calmodulin-dependent protein kinase kinase (CaMKK)β and liver kinase B1 (LKB1), the most-studied AMPKKs.

Here, through an examination of the mechanism by which SIRT1 level and activity are enhanced by atheroprotective PS in ECs, we report that CaMKKβ phosphorylates SIRT1 at Ser-27 and Ser-47 to increase its stability and activity. The translational significance of these findings is demonstrated by the increased atherosclerotic lesions in mouse lines with ablation of CaMKKβ or SIRT1.

Results

Shear Stress-Induced SIRT1 Depends on CaMKKβ. To establish a link between CaMKKβ and SIRT1 in the context of endothelium exposed to atheroprotective flow, we first examined CaMKKβ activation and its correlation with SIRT1 level in human umbilical

Significance

Different flow patterns in the arterial tree determine the severity and topographic distribution of atherosclerosis. Atheroprotective flow exerts anti-inflammatory and antioxidative effects on vascular endothelial cells, and the underlying mechanism involves the flow-induced upregulation of Sirtuin (SIRT)1. This study reveals that athero-protective flow activates Ca^{2+}/calmodulin-dependent protein kinase kinase (CaMKK)β, which, in turn, phosphorylates SIRT1 at Ser-27 and Ser-47 to increase the stability and activity of SIRT1. The mechanosensitive CaMKKβ-SIRT1 pathway alleviates inflammatory and redox status in the endothelium. Such a conclusion is evident from the drastically increased atherosclerosis in mice lacking CaMKKβ or endothelial SIRT1.

Author contributions: L.W., Z.C., D.A.J., Y.Z., S.C., and J.Y.-J.S. designed research; L.W., Z.C., F.Z., X.C., W.S., G.G.G., and Y.W. performed research; L.W., Y.Z., and J.Y.-J.S. analyzed data; and L.W., D.A.J., Y.Z., S.C., and J.Y.-J.S. wrote the paper.

The authors declare no conflict of interest.

[1]To whom correspondence may be addressed. E-mail: yizhuucr@yahoo.com, shuchien@ucsd.edu, or jshyy@ucsd.edu.

This article contains supporting information online at www.pnas.org/lookup/suppl/doi:10.1073/pnas.1309354110/-/DCSupplemental.

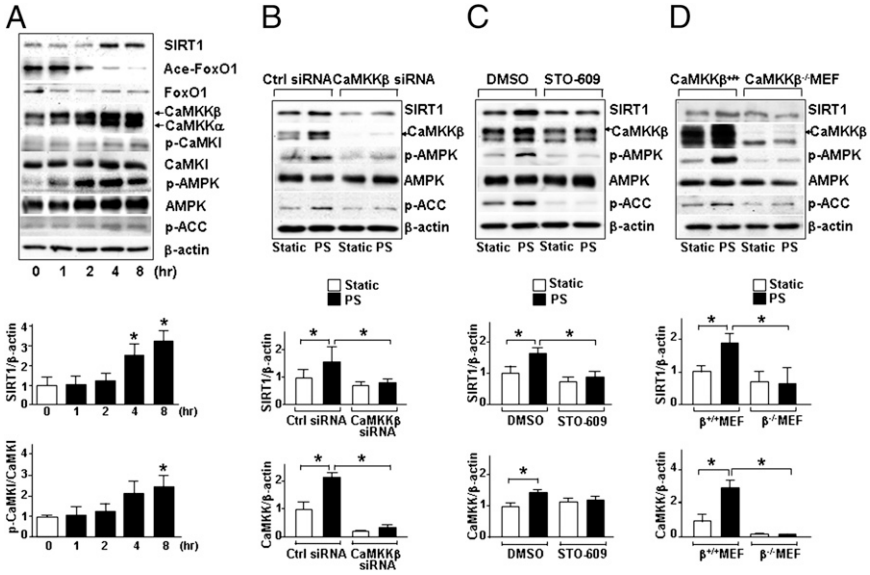

Fig. 1. CaMKKβ is required for SIRT1 induction in ECs under PS. (*A–C*) Immunoblots of HUVECs subjected to PS for the indicated time periods (*A*), pretreated with STO-609 (2.5 μg/mL) or DMSO for 30 min and then subjected to PS for 8 h (*B*), and transfected with control siRNA or CaMKKβ siRNA and then exposed to PS for 8 h or kept under static conditions for the same time (*C*). (*D*) Immunoblots of CaMKKβ$^{+/+}$ and CaMKKβ$^{-/-}$ MEFs exposed to static condition or PS for 8 h. The antibodies against targeted proteins are indicated for each immunoblot. Bar graphs below immunoblots summarize the means ± SEM of three independent experiments. *$P < 0.05$.

vein endothelial cells (HUVECs) subjected to PS. As illustrated in Fig. 1*A*, both CaMKKβ (the upper band recognized by an anti–pan-CaMKK) and SIRT1 levels were significantly elevated at 4 and 8 h after PS. As expected, there was an increase in phosphorylation of CaMKKβ targets [Ca^{2+}/calmodulin-dependent protein kinase (CaMK)I Thr-177 and AMPK Thr-172] and AMPK target [acetyl-CoA carboxylase (ACC) Ser 79]. Furthermore, the increased SIRT1 level was consistent with the decreased acetylation of FoxO1, a SIRT1 target. To test whether CaMKKβ mediates PS induction of SIRT1 and AMPK, CaMKKβ was knocked down by CaMKKβ siRNA or inhibited by STO-609, a CaMKK-specific inhibitor. Such CaMKKβ suppressions blocked the PS-induced increases in the levels of SIRT1 and AMPK phosphorylation (Fig. 1 *B* and *C*). The shear stress-dependent regulation of SIRT1 and AMPK was also abolished in CaMKKβ$^{-/-}$ murine embryonic fibroblasts (MEFs), compared with control CaMKKβ$^{+/+}$

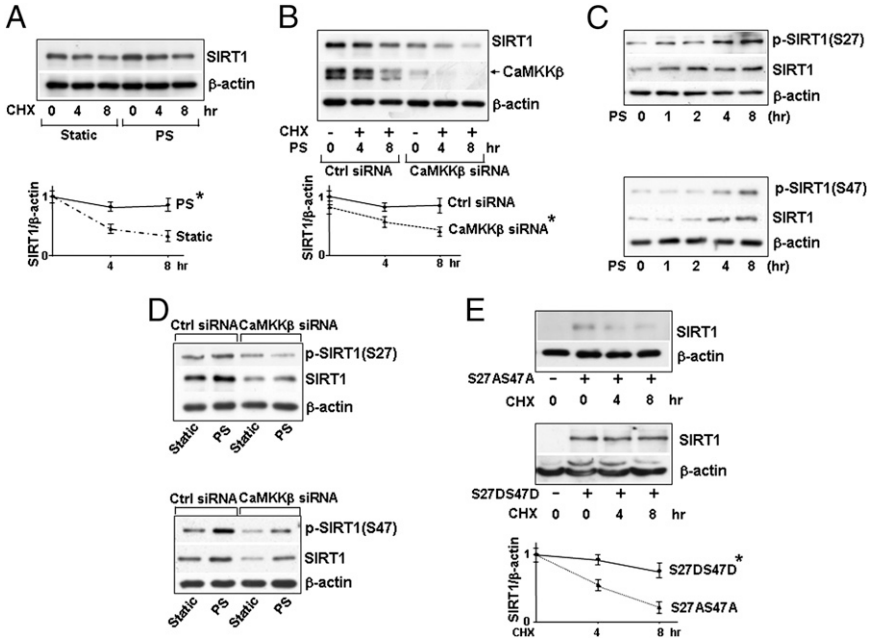

Fig. 2. PS increases SIRT1 stability via CaMKKβ phosphorylation at Ser-27 and Ser-47. Immunoblots of HUVECs pretreated with CHX (0.1 mg/mL) for 30 min before PS or kept under static conditions for the indicated time (*A* and *B*), transfected with or without control siRNA or CaMKKβ siRNA and then PS for 8 h (*B* and *C*), and transfected with control siRNA or CaMKKβ siRNA and then PS or static conditions for 8 h (*D*). (*E*) Immunoblots of lysed SIRT1$^{-/-}$ MEFs transfected with plasmid encoding SIRT1-S27AS47A or SIRT1-S27DS47D and then treated with CHX for the indicated times. The antibodies against targeted proteins are indicated. The plots below the immunoblots summarize the mean ± SEM results from three independent experiments. *$P < 0.05$.

MEFs (Fig. 1*D*). These results indicate that CaMKKβ plays a critical role in mediating the PS regulation of SIRT1.

CaMKKβ Phosphorylation of SIRT1 Enhances SIRT1 Stability. We then investigated the molecular basis by which PS increases the level of SIRT1. Because the mRNA level of SIRT1 did not change in ECs with the applied PS (Fig. S1*A*), we examined whether the elevated SIRT1 level was attributable to increased translation or protein stability. With translation inhibited by cycloheximide (CHX), the degradation rate of SIRT1 in ECs was significantly greater under static conditions than under PS (Fig. 2*A*), suggesting an increased SIRT1 stability under PS. This flow-associated effect was abolished with CaMKKβ knockdown (Fig. 2*B*). Because SIRT1 stability was reported to be affected by phosphorylation of its Ser-27 and Ser-47 residues (12), we investigated whether PS-increased SIRT1 stability was mediated via phosphorylation of SIRT1 at Ser-27 and Ser-47 and, if so, whether these modifications require CaMKKβ. As shown in Fig. 2*C*, PS increased the phosphorylation of SIRT1 Ser-27 and Ser-47, which was concomitant with increased SIRT1 level. Moreover, CaMKKβ siRNA knockdown greatly attenuated the phosphorylation of Ser-27 and Ser-47, both at the basal level and under PS (Fig. 2*D*). To further examine the role of Ser-27 and Ser-47 phosphorylation on SIRT1 stability, we overexpressed the phosphomimetic (i.e., SIRT1-S27D47D) or dephosphomimetic (i.e., SIRT1-S27AS47A) mutant in SIRT1$^{-/-}$ MEFs for CHX pulse-chase experiment. As shown in Fig. 2*E*, the exogenously expressed SIRT1-S27DS47D was more stable than SIRT1-S27AS47A. Taken together, these results indicate that PS increased

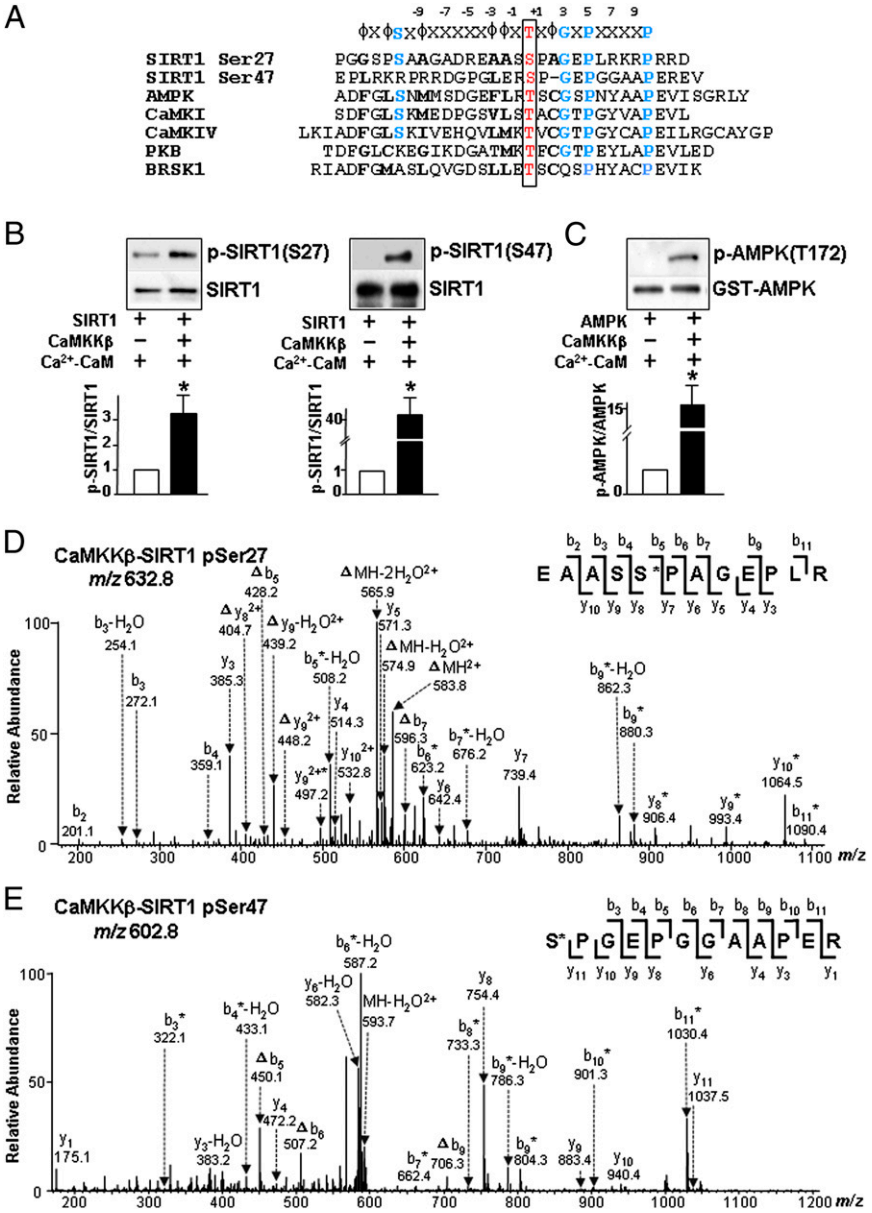

Fig. 3. CaMKKβ phosphorylates SIRT1 at Ser-27 and Ser-47. (*A*) Alignment of peptide sequences flanking SIRT1 Ser-27, SIRT1 Ser-47, AMPK Thr-172, CaMKI Thr-177, CaMKIV Thr-196, PKB Thr-308, and BRSK1 Thr-189. (*B* and *C*) Immunoblots of reaction products of mixtures of recombinant GST-CaMKKβ (50 ng) incubated with recombinant human SIRT1 (200 ng) (*B*) or AMPK (200 ng) (*C*) with 2 mM Ca^{2+} and recombinant calmodulin for 12 h (*B*) or for 30 min (*C*) at 30 °C. The phosphorylation of SIRT1 and AMPK was determined with the indicated antibodies. (*D* and *E*) MS/MS of phosphorylated SIRT1 tryptic peptides corresponding to residues 23–34 (EAASSPAGEPLR) (*D*) and 47–58 (SPGEPGGAAPER) (*E*) obtained from the kinase reaction mixtures described in *B* and analyzed by LC-MS/MS. The asterisk indicates that an ion bears a phosphate group, and neutral loss of an H_3PO_4 is represented by Δ.

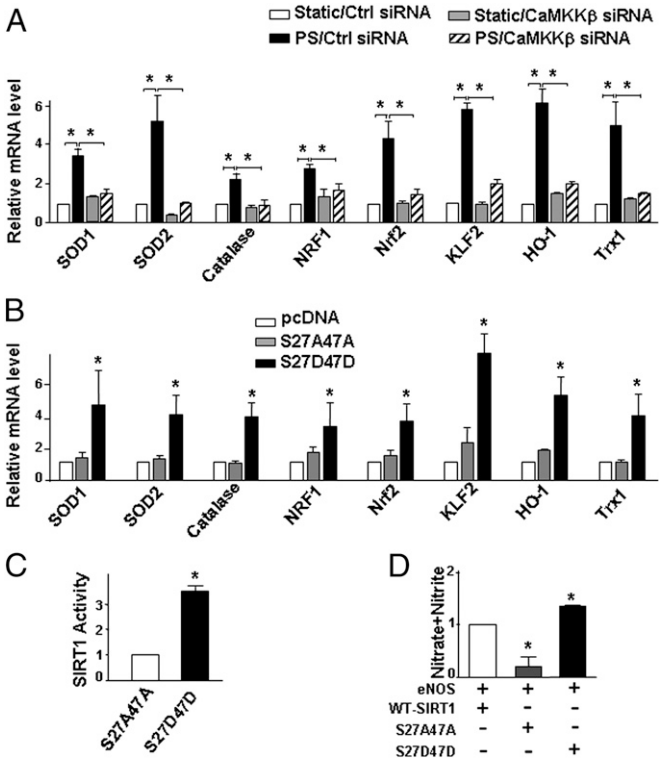

Fig. 4. Phosphorylation of SIRT1 Ser-27 and Ser-47 increases SIRT1 activity and expression of SIRT1 target genes. (*A* and *B*) Levels of SOD1, SOD2, catalase, NRF1, Nrf2, KLF2, HO-1, and Trx1 mRNA (relative to GAPDH) in HUVECs transfected with control siRNA or CaMKKβ siRNA (*A*) and in SIRT1$^{-/-}$ MEFs transfected with pcDNA, SIRT1-S27AS47A, or SIRT1-S27DS47D (*B*) and then exposed to PS or static conditions for 8 h. (*C* and *D*) SIRT1$^{-/-}$ MEFs were transfected with expression plasmids as indicated. Whole-cell lysates were collected for SIRT1 activity assays (*C*) and NO bioavailability expressed as NOx (*D*). *$P < 0.05$.

SIRT1 stability and that this was associated with phosphorylation of SIRT1 at Ser-27 and Ser-47 and dependent upon CaMKKβ.

CaMKKβ Phosphorylates SIRT1 at Ser-27 and Ser-47. CaMKKβ phosphorylates AMPK at Thr-172, CaMKI at Thr-177, Ca^{2+}/calmodulin-dependent protein IV (CaMKIV) at Thr-196, protein kinase B (PKB) at Thr-308, and BR serine/threonine kinase (BRSK)1 at Thr-189 (18-22). Homology among amino acid sequences adjacent to SIRT1 Ser-27, Ser-47, and the respective CaMKKβ phosphorylation sites of AMPK, CaMKI, CaMKIV, PKB, and BRSK1 (Fig. 3*A*) indicates that CaMKKβ could be a SIRT1 kinase. To verify this, we first performed in vitro kinase assay using recombinant SIRT1 and CaMKKβ. In the presence of Ca^{2+}/CaM, SIRT1 phosphorylation at both Ser-27 and Ser-47 was increased (Fig. 3*B*). As a positive control, AMPK phosphorylation at Thr-172 was increased as well (Fig. 3*C*). Additionally, nano-liquid chromatography/tandem mass spectrometry (nano–LC-MS/MS) analysis confirmed that CaMKKβ can phosphorylate Ser-27 and Ser-47. The phosphorylation of SIRT1 at Ser-27 and Ser-47 within the corresponding tryptic peptides was verified by characteristic neutral loss of a phosphoric acid group (98 Da) (Fig. 3 *D* and *E*). In addition, the sites of phosphorylation were supported by characteristic sequence ions (y and b ions) observed in the MS/MS (Tables S1 and S2). Thus, CaMKKβ can directly phosphorylate SIRT1 at Ser-27 and Ser-47.

PS Up-Regulates Antioxidative and Anti-inflammatory Genes via CaMKKβ-SIRT1. Like SIRT1, PS exerts antioxidative and anti-inflammatory effects on ECs, in part, by up-regulation of anti-oxidative and anti-inflammatory genes (2, 23, 24). In our flow channel experiments, PS increased the mRNA level of superoxide dismutase (SOD)1, SOD2, catalase, nuclear respiratory factor 1 (NRF1), nuclear factor erythroid 2-related factor 2 (Nrf2), Krüppel-like factor (KLF)2, heme oxygenase (HO)-1, and thioredoxin (Trx)1 in ECs, which are involved in the SIRT1-regulated antioxidative effect (25–30). More importantly, CaMKKβ knockdown abolished this effect of PS (Fig. 4*A*). To establish that CaMKKβ phosphorylation of SIRT1 mediates the induction of these antioxidative and anti-inflammatory genes, we compared mRNA levels of these genes in SIRT1$^{-/-}$ MEFs transfected with pcDNA control vector, SIRT1-S27AS47A, or SIRT1-S27DS47D. Levels of all these mRNAs were higher in MEFs transfected with SIRT1-S27DS47D than pcDNA or SIRT1-S27AS47A (Fig. 4*B*). In parallel, MEFs transfected with SIRT1-S27DS47D showed increased SIRT1 activity (Fig. 4*C*). Because SIRT1 deacetylates eNOS with attendant increase in eNOS activity (5), MEFs expressing SIRT1-S27DS47D also showed enhanced eNOS-derived NO (Fig. 4*D*).

CaMKKβ Knockout Increases Oxidative Stress and Inflammation in the Arterial Wall. To extrapolate the findings from flow channel experiments to in vivo conditions, we examined whether the levels of total SIRT1 and phosphorylated SIRT1 vary by location in the

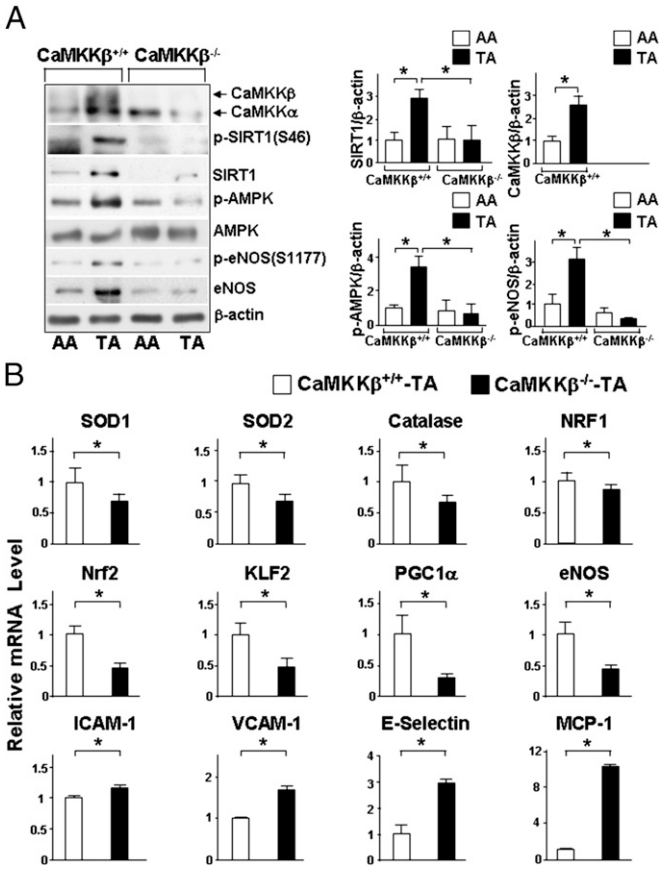

Fig. 5. CaMKKβ and SIRT1 are involved in the regulation of antioxidative and anti-inflammatory genes in mouse aorta. (*A*) Immunoblots of tissue lysates from the aortic arch (AA) and the thoracic aorta (TA) isolated from CaMKKβ$^{+/+}$ mice and their CaMKKβ$^{-/-}$ littermates performed with indicated antibodies. Bar graphs to the right summarize the means ± SEM from six mice in each group. (*B*) Levels of SOD1, SOD2, catalase, NRF1, Nrf2, KLF2, PGC1α, eNOS, ICAM-1, VCAM-1, E-selectin, and MCP-1 mRNA (relative to GADPH) in TA from CaMKKβ$^{-/-}$ and their CaMKKβ$^{+/+}$ littermates. The results summarize the means ± SEM from 15 mice in each group. *$P < 0.05$.

arterial tree as a function of flow pattern and, if so, whether CaMKKβ is involved. Because mouse SIRT1 has a glutamine at residue 27 and a serine at residue 46 (homologous to human Ser-47), only phosphorylation at Ser-46 was monitored for the mouse studies. Wild-type, namely CaMKKβ$^{+/+}$ mice, showed higher levels of SIRT1, phosphorylated SIRT1 at Ser-46 and phosphorylated AMPK at Thr-172 in the thoracic aorta, which is exposed to atheroprotective flow, compared with the aortic arch, which is under atheroprone flow (Fig. 5*A*). Importantly, CaMKKβ$^{-/-}$ littermates did not show increased SIRT1 expression or phosphorylation of SIRT1 or AMPK in thoracic aortas. In addition, we performed *en face* staining on the aortic arch and thoracic aorta of CaMKKβ$^{+/+}$ or CaMKKβ$^{-/-}$ mice to compare the expression levels of CaMKKβ and SIRT1. As shown in Fig. S2, the thoracic aorta of CaMKKβ$^{+/+}$ mice exhibited higher levels of anti-CaMKKβ and anti-SIRT1 staining than the aortic arch. However, in CaMKKβ$^{-/-}$ mice, the staining for both anti-CaMKKβ and anti-SIRT1 was weak and not significantly different between thoracic aorta and aortic arch. Taken together, these data indicated that the expression of SIRT1 in the arterial tree was regulated by the local flow patterns in a CaMKKβ-dependent manner.

Consistent with the antioxidative and anti-inflammatory effects of atheroprotective flow, the mRNA levels of the atheroprotective gene products SOD1, SOD2, catalase, NRF1, Nrf2, PGC1α, and eNOS were significant lower in the thoracic aorta of CaMKKβ$^{-/-}$ mice compared with those in CaMKKβ$^{+/+}$ mice (Fig. 5*B*). Conversely, the mRNA levels of intercellular adhesion molecule (ICAM)-1, vascular cell adhesion molecule (VCAM)-1, E-selectin, and monocyte chemotactic protein (MCP)-1 were higher in the thoracic aorta of CaMKKβ$^{-/-}$ mice (Fig. 5*B*). Higher levels of ICAM-1, VCAM-1, E-selectin, and MCP-1 were also found in PS-treated ECs in which CaMKKβ had been knocked down (Fig. S3). Thus, CaMKKβ ablation led to prooxidative and proinflammatory states in vivo and in vitro.

CaMKKβ-SIRT1 Is Antiatherogenic in Mouse Arterial Walls. The results in Figs. 1–5 indicate that the CaMKKβ-SIRT1 pathway maintains an antioxidative and anti-inflammatory phenotype of ECs. Therefore, we compared the topographic distribution and severity of atherosclerosis in mice with ablation of CaMKKβ or SIRT1. CaMKKβ$^{-/-}$ mice were crossed with apolipoprotein (Apo)E$^{-/-}$ to generate CaMKKβ$^{-/-}$/ApoE$^{-/-}$ and their CaMKKβ$^{+/+}$/ApoE$^{-/-}$ littermates. In parallel, EC-SIRT1$^{+/+}$/ApoE$^{-/-}$ and EC-SIRT1$^{-/-}$/ApoE$^{-/-}$ mouse lines were also obtained. After receiving a Paigen diet for 9 wk, mice were killed and *en face* staining was performed on the aortic specimens. As illustrated in Fig. 6 *A* and *B*, the total lesion area was 2.2-fold greater in CaMKKβ$^{-/-}$/ApoE$^{-/-}$ than CaMKKβ$^{+/+}$/ApoE$^{-/-}$ mice. The lesion areas in the aortic arch and thoracic aorta were 12 ± 1.4% and 1.6 ± 0.2%, respectively, for CaMKKβ$^{+/+}$/ApoE$^{-/-}$ mice and 18 ± 2.8% and 5.7 ± 0.6%, respectively, for CaMKKβ$^{-/-}$/ApoE$^{-/-}$ mice (Fig. 6*B*). Notably, the serum levels of total cholesterol and low-density lipoprotein were similar for the two mouse groups (Table S3). Compared with EC-SIRT1$^{+/+}$/ApoE$^{-/-}$ mice, diploid *SIRT1* deficiency in the endothelium caused a 2.4-fold increase in atherosclerosis (Fig. 6 *C* and *D*). The lesion areas in the aortic arch and thoracic aorta were 10 ± 1.9% and 1.5 ± 0.3%, respectively, for EC-SIRT1$^{+/+}$/ApoE$^{-/-}$ mice and 21 ± 3.5% and 5.7 ± 1.2%, respectively, for EC-SIRT1$^{-/-}$/ApoE$^{-/-}$ mice. Similar to CaMKKβ knockout, SIRT1 ablation in the endothelium did not alter the lipid profile (Table S4). In all, CaMKKβ ablation in connection with decreased SIRT1 expression in the endothelium increase atherosclerosis in mouse aorta, which suggests the atheroprotective role of flow-induced CaMKKβ-SIRT1.

Discussion

The principal findings of this study are that (*i*) CaMKKβ phosphorylates SIRT1 at Ser-27 and Ser-47 in response to atheroprotective PS in ECs, (*ii*) phosphorylation of SIRT1 at Ser-27 and Ser-47 promotes SIRT1 stability and deacetylase activity, and (*iii*)

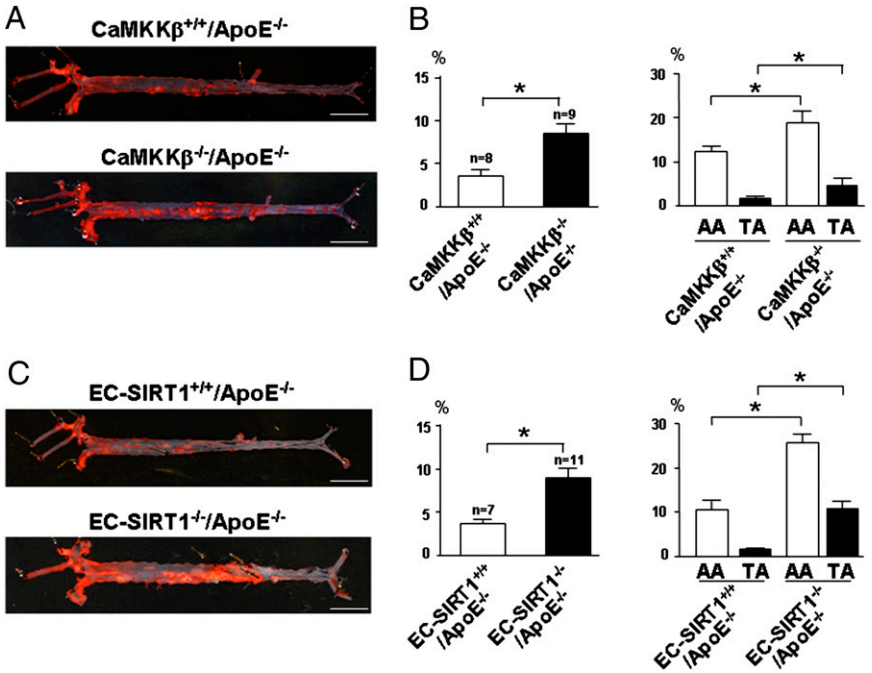

Fig. 6. CaMKKβ and SIRT1 ablation enhances atherogenesis in mouse aorta. Macrophotographs of oil red O-stained aorta from CaMKKβ$^{+/+}$ApoE$^{-/-}$ and CaMKKβ$^{-/-}$ApoE$^{-/-}$ mice (*A*) and EC-SIRT1$^{+/+}$/ApoE$^{-/-}$ and EC-SIRT1$^{-/-}$/ApoE$^{-/-}$ mice (*C*) fed a Paigen diet for 9 wk and killed. (Scale bar: 0.5 cm.) (*B* and *D*) Quantification of percentage of lesion areas in the whole aorta (*Left*) and aortic arch (AA) and thoracic aorta (TA) (*Right*). *$P < 0.05$; n denotes the number of animals used.

ablation of either CaMKKβ or endothelial SIRT1 increases atherosclerosis in mice.

CaMKKβ can be activated by both Ca^{2+}/CaM-dependent and -independent mechanisms (31). Shear stress is well documented to increase intracellular $[Ca^{2+}]$ ($[Ca^{2+}]_i$) in ECs, caused by both Ca^{2+} influx and endoplasmic reticulum release. The combination of both mechanisms can maintain $[Ca^{2+}]_i$ at twice the basal level for about 1,000 s (32), an interval consistent with posttranslational modifications of signaling molecules such as AMPK (a downstream target of CaMKKβ) in ECs responding to PS (Fig. 1 and ref. 33). PS can increase expression of CaMKKβ through an augmentation of CaMKKβ stability from autophosphorylation (34, 35), as well as an increase of CaMKKβ transcription, as shown in the current study, both in the flow channel in vitro and in the thoracic aorta in vivo (Fig. S1 *C* and *D*).

Because the SIRT1 mRNA level does not increase in ECs under PS, nor does it differ significantly between aortic arch and thoracic aorta (Fig. S1 *A* and *B*), the PS-induced SIRT1 does not seem to involve transcriptional activation. CaMKKβ phosphorylation of SIRT1 at Ser-27 and Ser-47 contributes to the enhanced SIRT1 stability in ECs under PS. We have shown previously that shear-stress activation of AMPK involves LKB1 (36). However, LKB1 knockdown has little effect on the PS-induced SIRT1 level (Fig. S4*A*). Furthermore, both of the amino acid sequences flanking Ser-27 and Ser-47 do not align well with the phosphorylation consensus sequence of LKB1 (Fig. S4*B*), suggesting that SIRT1 is not a LKB1 substrate. Rather, SIRT1 appears to be upstream of LKB1, because SIRT1 has been shown to modulate the activity of LKB1 (37). Thus, CaMKKβ and LKB1 both can regulate AMPK, but only CaMKKβ phosphorylates SIRT1. In addition to CaMKKβ, several other kinases, including JNK1, JNK2, and CDK5, can phosphorylate SIRT1 at Ser-27 and Ser-47 (11–13). However, JNK and CDK5 are unlikely to be involved in PS-induced SIRT1 Ser-27 and Ser-47 phosphorylation because pharmacological inhibition of JNK or CDK5 does not affect PS induction of SIRT1 in ECs (Fig. S4 *C* and *D*). Given that human SIRT1 has more than 10 putative phosphorylation sites (7), different stimuli may activate distinct sets of kinases, which would result in various patterns of posttranslational modifications of SIRT1. The lack of involvement of CDK5 and JNK in PS-induced SIRT1 phosphorylation is also supported by the observations that PS increases SIRT1 in cytoplasm, whereas CDK5-dependent phosphorylation of SIRT1 occurs in the nucleus. Furthermore, disturbed flow, but not atheroprotective flow, activates JNK (38).

At the tissue level, the atheroprotective role of the CaMKKβ-SIRT1 axis is demonstrated by increased atherosclerosis in the thoracic aorta of CaMKKβ$^{-/-}$/ApoE$^{-/-}$ and EC-SIRT1$^{-/-}$/ApoE$^{-/-}$ mice compared with the respective wild-type mice. Although CaMKKβ$^{-/-}$/ApoE$^{-/-}$ have a systemic CaMKKβ knockout, it is to be noted that EC-restricted ablation of SIRT1 in EC-SIRT1$^{-/-}$/ApoE$^{-/-}$ mice confers a similar phenotype in terms of increased atherosclerosis in the normally atheroprotective areas. It is also noteworthy that the serum lipid profiles in mice were not affected by the ablation of CaMKKβ or SIRT1 (Tables S3 and S4). These findings indicate that the increased atherosclerosis in CaMKKβ$^{-/-}$/ApoE$^{-/-}$ and EC-SIRT1$^{-/-}$/ApoE$^{-/-}$ mice most likely resulted from the increased inflammatory and oxidative stress in the endothelium attributable to the lack of CaMKKβ-SIRT1 signaling axis, rather than through lipid changes. Noticeably, the lung ECs in EC-SIRT1$^{-/-}$ mice had negligible SIRT1 level in comparison with that in EC-SIRT1$^{+/+}$ mice. In contrast, SIRT1 level in macrophages in EC-SIRT1$^{-/-}$ mice was only moderately lower than that in EC-SIRT1$^{+/+}$ mice. Thus, the mildly decreased level of SIRT1 in hematopoietic cells in EC-SIRT1$^{-/-}$/ApoE$^{-/-}$ mice may also contribute to the increased atherosclerosis, although to a much lesser extent than that in ECs. This conclusion is supported by a previous study demonstrating that SIRT1 overexpression in the endothelium ameliorated atherosclerosis in mouse aorta (4).

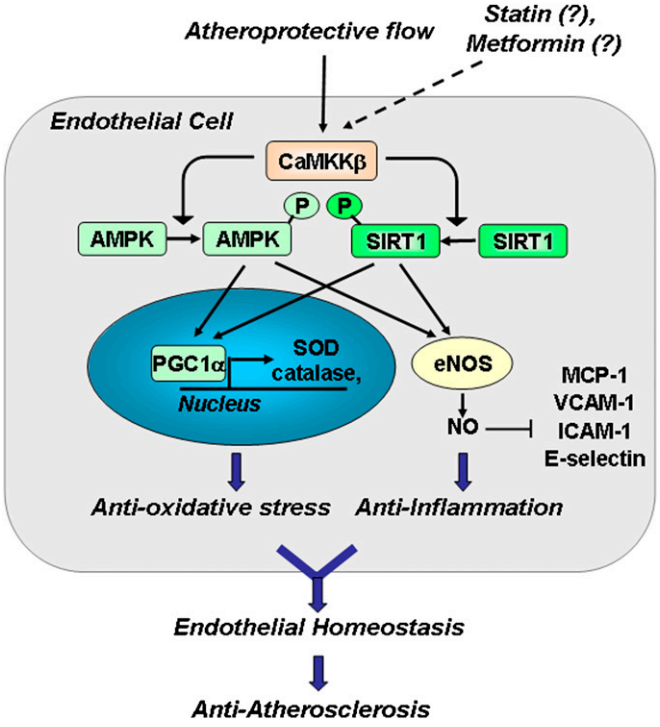

Fig. 7. Graphic summary for the antioxidative and anti-inflammatory effects of CaMKKβ phosphorylation of SIRT1 in ECs responding to atheroprotective flow. Together, AMPK and SIRT1 activate PGC1α in the nucleus, leading to up-regulation of antioxidant enzymes such as SOD and catalase. AMPK and SIRT1 also act in concert in the cytoplasm to activate eNOS and augment eNOS-derived NO to exert an anti-inflammatory effects by repressing MCP-1, VCAM-1, ICAM-1, and E-selectin. Collectively, the coregulation of AMPK and SIRT1 by CaMKKβ contributes to endothelial homeostasis and an atheroprotective phenotype of ECs.

Our finding that CaMKKβ is a common kinase to two master regulators, SIRT1 and AMPK, in ECs that respond to shear stress suggests that CaMKKβ is a key upstream regulator of EC homeostasis by coregulating AMPK and SIRT1. This thesis is supported by the increased atherosclerosis in CaMKKβ$^{-/-}$, EC-SIRT1$^{-/-}$, and AMPKα2$^{-/-}$ mice with an ApoE-deficient background (Fig. 6 and Fig. S5). In addition to atheroprotective flow, statins and metformin induce SIRT1 in ECs (39, 40), and CaMKKβ mediates the activation of AMPK by statins (41). Thus, our findings indicate the involvement of the defined CaMKKβ-AMPK/SIRT1 pathway in the beneficial responses to various atheroprotective physicochemical stimuli (Fig. 7).

Materials and Methods

Cell Culture, Transfections, and Shear-Stress Experiments. HUVECs at 50–70% confluence were transfected with CaMKKβ siRNA (Qiagen; SI0259713) or control siRNA (10 nM) with the use of Lipofectamine 2000 RNAi Max (Invitrogen). SIRT1-null MEFs were transfected with CMV promoter-driven wild-type SIRT1, SIRT1 S27AS47A (a gift from Ulrich Mahlknecht, University Medical Center, Homburg/Saar, Germany), or S27DS47D mutant for 48 h before use. PS with a shear stress of 12 ± 4 dyn/cm^2 was generated by a circulating flow system and a reciprocating syringe pump to introduce a sinusoidal component with a frequency of 1 Hz onto the shear stress.

Immunoblot and Quantitative PCR Analyses. Antibodies against pan-AMPK, phospho-AMPK Thr-172, pan-ACC, phospho-ACC Ser-79, SIRT1, phospho-SIRT1 Ser-27, phospho-SIRT1 Ser-47, eNOS, FoxO1, and horseradish peroxidase-conjugated anti-rabbit and anti-mouse IgG were from Cell Signaling. Antibody against pan-CaMKK was from BD Biosciences Pharmingen. Anti–β-actin,

anti-acetyl FoxO1 Lys-271, and anti-phospho-CaMKI Thr-177 antibodies were from Santa Cruz Biotechnology. Quantitative PCR was performed by the iCycler Realtime PCR Detection System (Bio-Rad).

CaMKKβ Kinase and SIRT1 Deacetylase Activity and NO Bioavailability Assays. Recombinant SIRT1 and CaMKKβ (Sigma Aldrich) were mixed and incubated in a reaction buffer containing 50 mM Hepes (pH 7.4), 5 mM $MgCl_2$, 200 μM ATP, 200 μM AMP, 2 mM $CaCl_2$, and 2 μM calmodulin for 12 h at 30 °C. The reaction was terminated by the addition of SDS loading buffer. For SIRT1 deacetylase activity assay, whole-cell extracts were incubated with Fluor-de-Lys-SIRT1 as the substrate (42). The deacetylation of the substrate was measured by use of a microplate-reading fluorometer, with excitation and emission set at 380 and 460 nm, respectively. The NO production from cells was detected as accumulated nitrite/nitrate in the cell culture media by using nitrite/nitrate fluorometric assay (Cayman Chemicals).

Nano–LC-MS/MS. The reaction mixtures from an in vitro kinase assay were resolved with 12% (wt/vol) SDS/PAGE. The gel bands containing SIRT1 were excised, and proteins were reduced in-gel with DTT, alkylated with iodoacetamide, and digested with trypsin at 37 °C for 16 h. Peptides were extracted with 5% acetic acid in H_2O and then 5% acetic acid in CH_3CN/H_2O (1:1; vol/vol). Online LC-MS/MS analysis was performed with an LTQ-Orbitrap Velos mass spectrometer coupled with the EASY n-LCII HPLC system and a nanoelectrospray ionization source (Thermo Scientific) for peptide sequencing and phosphorylation identification. The LC-MS/MS data were used for the identification of phosphorylation sites by use of Mascot Server 2.2 (Matrix Science) and searching the mass-to-charge ratio data files against the National Center for Biotechnology Information database.

Mouse Models. The animal experimental protocols were approved by the University of California, Riverside Institutional Animal Care and Use Committee. $ApoE^{-/-}$, SIRT1 floxed (SIRT1 $flox^{+/+}$), and Tek-Cre^{Tg} mice with a C57BL/6 background were from The Jackson Laboratory. The CaMKK$\beta^{-/-}$ mouse line was a gift from Talal Chatila (University of California, Los Angeles, CA). The SIRT1 $flox^{+/+}$ mice in a C57BL/6 background were bred with Tek-Cre^{Tg} mice to generate the EC-specific SIRT1-knockout (EC-$SIRT1^{-/-}$) mice with the genotype of SIRT1 $flox^{+/+}$/Cre^{Tg}. Heterozygotic SIRT1 $flox^{+/-}$/Cre^{Tg} line was used to generate EC-$SIRT1^{-/-}$ mice and their wild-type littermates (SIRT1 $flox^{-/-}$/Cre^{Tg}, SIRT1 $flox^{+/+}$, and SIRT1 $flox^{-/-}$). AMPKα$2^{-/-}$$ApoE^{-/-}$ and CaMKK$\beta^{-/-}$$ApoE^{-/-}$ mice were generated by crossing AMPKα$2^{-/-}$ or CaMKK$\beta^{-/-}$ with $ApoE^{-/-}$ mice. EC-SIRT1–null mice with an $ApoE^{-/-}$ background (EC-$SIRT1^{-/-}$/$ApoE^{-/-}$) were generated by crossbreeding SIRT1 $flox^{+/+}$ or Tek-Cre^{Tg} line with $ApoE^{-/-}$ mice to obtain SIRT1 $flox^{+/+}$/$ApoE^{-/-}$ and Tek-Cre^{Tg}/$ApoE^{-/-}$ mice, respectively. These two strains were then crossbred to generate SIRT1 $flox^{+/+}$/Tek-Cre^{Tg}/$ApoE^{-/-}$ mice and wild-type SIRT1 littermates with null ApoE.

Assessment of Atherosclerosis. Six- to eight-week-old male CaMKK$\beta^{-/-}$/$ApoE^{-/-}$, AMPKα$2^{-/-}$/$ApoE^{-/-}$, and EC-$SIRT1^{-/-}$/$ApoE^{-/-}$ mice and their littermates were fed a high-fat, high-cholesterol Paigen diet containing 15% fat, 1.25% cholesterol, and 0.5% sodium cholate (TD.88051; Harlan Teklad) ad libitum for the indicated time and then were killed. Aortas were isolated to assess lesion formation and distribution by oil red O staining.

***En Face* Immunofluorescent Staining and Confocal Scanning.** Six- to eight-week-old CaMKK$\beta^{+/+}$ or CaMKK$\beta^{-/-}$ mice were killed, and aortas were dissected and fixed in 4% paraformaldehyde in PBS for 1 h and then 0.5% Triton and 0.1% SDS for 30 min. The specimens were blocked with 2% BSA for 1 h before the application of antibody against CaMKKβ (Santa Cruz Biotechnology) and SIRT1 (Cell Signaling) at a concentration of 1:200 for 12 h. Alexa Fluor 488 goat anti-mouse IgG and rhodamine (TRITC)-conjugated goat anti-rabbit IgG were used as respective secondary antibodies with a concentration of 1:200 in PBS, whereas the nuclei were stained with DAPI. Images of *en face* staining were acquired using an Olympus FV1000 confocal microscope. The zoom-in ratio was set to be 4. DAPI, FITC, and TRITC fluorophores were excited at 405, 488, and 559 nm at laser power of 0.3%, 2%, and 1%.

Statistical Analysis. Data are given as means ± SEM averaged from independent experiments or aortic specimens as noted. Comparisons between two groups were evaluated by two-tailed Student *t* test or among more than two groups by ANOVA with Bonferroni or Tukey post hoc test. $P < 0.05$ was considered statistically significant.

ACKNOWLEDGMENTS. This work was supported in part by National Institutes of Health Grants HL89940 and HL105318 (to J.Y.-J.S.), DK82779 (to Y.W.), HL108735 (to S.C.) and National Natural Science Foundation of China Grant 81130002 (to Y.Z.).

1. Chen Z, et al. (2010) Shear stress, SIRT1, and vascular homeostasis. *Proc Natl Acad Sci USA* 107(22):10268–10273.
2. Potente M, Dimmeler S (2008) Emerging roles of SIRT1 in vascular endothelial homeostasis. *Cell Cycle* 7(14):2117–2122.
3. Potente M, et al. (2007) SIRT1 controls endothelial angiogenic functions during vascular growth. *Genes Dev* 21(20):2644–2658.
4. Zhang QJ, et al. (2008) Endothelium-specific overexpression of class III deacetylase SIRT1 decreases atherosclerosis in apolipoprotein E-deficient mice. *Cardiovasc Res* 80(2):191–199.
5. Mattagajasingh I, et al. (2007) SIRT1 promotes endothelium-dependent vascular relaxation by activating endothelial nitric oxide synthase. *Proc Natl Acad Sci USA* 104(37):14855–14860.
6. Kwon HS, Ott M (2008) The ups and downs of SIRT1. *Trends Biochem Sci* 33(11): 517–525.
7. Sasaki T, et al. (2008) Phosphorylation regulates SIRT1 function. *PLoS ONE* 3(12): e4020.
8. Yang Y, et al. (2007) SIRT1 sumoylation regulates its deacetylase activity and cellular response to genotoxic stress. *Nat Cell Biol* 9(11):1253–1262.
9. Yamakuchi M (2012) MicroRNA regulation of SIRT1. *Front Physiol* 3:68.
10. Lee J, Kemper JK (2010) Controlling SIRT1 expression by microRNAs in health and metabolic disease. *Aging (Albany, NY Online)* 2(8):527–534.
11. Nasrin N, et al. (2009) JNK1 phosphorylates SIRT1 and promotes its enzymatic activity. *PLoS ONE* 4(12):e8414.
12. Ford J, Ahmed S, Allison S, Jiang M, Milner J (2008) JNK2-dependent regulation of SIRT1 protein stability. *Cell Cycle* 7(19):3091–3097.
13. Bai B, et al. (2012) Cyclin-dependent kinase 5-mediated hyperphosphorylation of sirtuin-1 contributes to the development of endothelial senescence and atherosclerosis. *Circulation* 126(6):729–740.
14. Back JH, et al. (2011) Cancer cell survival following DNA damage-mediated premature senescence is regulated by mammalian target of rapamycin (mTOR)-dependent Inhibition of sirtuin 1. *J Biol Chem* 286(21):19100–19108.
15. Ruderman NB, et al. (2010) AMPK and SIRT1: A long-standing partnership? *Am J Physiol Endocrinol Metab* 298(4):E751–E760.
16. Timmers S, et al. (2011) Calorie restriction-like effects of 30 days of resveratrol supplementation on energy metabolism and metabolic profile in obese humans. *Cell Metab* 14(5):612–622.
17. Cantó C, et al. (2009) AMPK regulates energy expenditure by modulating NAD+ metabolism and SIRT1 activity. *Nature* 458(7241):1056–1060.
18. Woods A, et al. (2005) Ca2+/calmodulin-dependent protein kinase kinase-beta acts upstream of AMP-activated protein kinase in mammalian cells. *Cell Metab* 2(1):21–33.
19. Matsushita M, Nairn AC (1998) Characterization of the mechanism of regulation of Ca2+/ calmodulin-dependent protein kinase I by calmodulin and by Ca2+/calmodulin-dependent protein kinase kinase. *J Biol Chem* 273(34):21473–21481.
20. Yano S, Tokumitsu H, Soderling TR (1998) Calcium promotes cell survival through CaM-K kinase activation of the protein-kinase-B pathway. *Nature* 396(6711): 584–587.
21. Fujimoto T, et al. (2008) Activation of SAD kinase by Ca2+/calmodulin-dependent protein kinase kinase. *Biochemistry* 47(13):4151–4159.
22. Tokumitsu H, Soderling TR (1996) Requirements for calcium and calmodulin in the calmodulin kinase activation cascade. *J Biol Chem* 271(10):5617–5622.
23. Pfluger PT, Herranz D, Velasco-Miguel S, Serrano M, Tschöp MH (2008) Sirt1 protects against high-fat diet-induced metabolic damage. *Proc Natl Acad Sci USA* 105(28):9793–9798.
24. Csiszar A, et al. (2009) Anti-oxidative and anti-inflammatory vasoprotective effects of caloric restriction in aging: Role of circulating factors and SIRT1. *Mech Ageing Dev* 130(8):518–527.
25. Csiszar A, et al. (2009) Resveratrol induces mitochondrial biogenesis in endothelial cells. *Am J Physiol Heart Circ Physiol* 297(1):H13–H20.
26. Xia N, et al. (2010) Resveratrol reverses endothelial nitric-oxide synthase uncoupling in apolipoprotein E knockout mice. *J Pharmacol Exp Ther* 335(1):149–154.
27. Gracia-Sancho J, Villarreal G, Jr., Zhang Y, García-Cardeña G (2010) Activation of SIRT1 by resveratrol induces KLF2 expression conferring an endothelial vasoprotective phenotype. *Cardiovasc Res* 85(3):514–519.
28. Ungvari Z, et al. (2010) Resveratrol confers endothelial protection via activation of the antioxidant transcription factor Nrf2. *Am J Physiol Heart Circ Physiol* 299(1): H18–H24.
29. Alcendor RR, et al. (2007) Sirt1 regulates aging and resistance to oxidative stress in the heart. *Circ Res* 100(10):1512–1521.
30. Thirunavukkarasu M, et al. (2007) Resveratrol alleviates cardiac dysfunction in streptozotocin-induced diabetes: Role of nitric oxide, thioredoxin, and heme oxygenase. *Free Radic Biol Med* 43(5):720–729.
31. Tokumitsu H, Iwabu M, Ishikawa Y, Kobayashi R (2001) Differential regulatory mechanism of Ca2+/calmodulin-dependent protein kinase kinase isoforms. *Biochemistry* 40(46):13925–13932.
32. Liu B, Lu S, Zheng S, Jiang Z, Wang Y (2011) Two distinct phases of calcium signalling under flow. *Cardiovasc Res* 91(1):124–133.

33. Young A, et al. (2009) Flow activation of AMP-activated protein kinase in vascular endothelium leads to Krüppel-like factor 2 expression. *Arterioscler Thromb Vasc Biol* 29(11):1902–1908.
34. Tokumitsu H, Hatano N, Fujimoto T, Yurimoto S, Kobayashi R (2011) Generation of autonomous activity of Ca(2+)/calmodulin-dependent protein kinase kinase β by autophosphorylation. *Biochemistry* 50(38):8193–8201.
35. Green MF, et al. (2011) Ca2+/Calmodulin-dependent protein kinase kinase beta is regulated by multisite phosphorylation. *J Biol Chem* 286(32):28066–28079.
36. Zhang Y, et al. (2006) AMP-activated protein kinase is involved in endothelial NO synthase activation in response to shear stress. *Arterioscler Thromb Vasc Biol* 26(6): 1281–1287.
37. Lan F, Cacicedo JM, Ruderman N, Ido Y (2008) SIRT1 modulation of the acetylation status, cytosolic localization, and activity of LKB1. Possible role in AMP-activated protein kinase activation. *J Biol Chem* 283(41):27628–27635.
38. Cuhlmann S, et al. (2011) Disturbed blood flow induces RelA expression via c-Jun N-terminal kinase 1: A novel mode of NF-κB regulation that promotes arterial inflammation. *Circ Res* 108(8):950–959.
39. Zheng Z, et al. (2012) Sirtuin 1-mediated cellular metabolic memory of high glucose via the LKB1/AMPK/ROS pathway and therapeutic effects of metformin. *Diabetes* 61(1):217–228.
40. Ota H, et al. (2010) Induction of endothelial nitric oxide synthase, SIRT1, and catalase by statins inhibits endothelial senescence through the Akt pathway. *Arterioscler Thromb Vasc Biol* 30(11):2205–2211.
41. Kou R, Sartoretto J, Michel T (2009) Regulation of Rac1 by simvastatin in endothelial cells: Differential roles of AMP-activated protein kinase and calmodulin-dependent kinase kinase-beta. *J Biol Chem* 284(22):14734–14743.
42. Vaziri H, et al. (2001) hSIR2(SIRT1) functions as an NAD-dependent p53 deacetylase. *Cell* 107(2):149–159.